

Supplementary Materials to:

An Adoption of the Fractional Maxwell Model for Characterizing the Interfacial Dilational Viscoelasticity of Complex Surfactant Systems

Giuseppe Loglio ^{1,*}, Agnieszka Czakaj ², Ewelina Jarek ², Volodymyr I. Kovalchuk ^{3,*}, Marcel Krzan ², Libero Liggieri ¹, Reinhard Miller ⁴ and Piotr Warszynski ²

¹ Institute of Condensed Matter Chemistry and Technologies for Energy (ICMATE-CNR), unit of Genova, 16149 Genoa, Italy; libero.liggieri@ge.icmate.cnr.it

² Jerzy Haber Institute of Catalysis and Surface Chemistry, Polish Academy of Sciences, 30-239 Krakow, Poland; czakaja@gmail.com (A.C.); ewelina.jarek@ikifp.edu.pl (E.J.); marcel.krzan@ikifp.edu.pl (M.K.); piotr.warszynski@ikifp.edu.pl (P.W.)

³ Institute of Biocolloid Chemistry, National Academy of Sciences of Ukraine, 03680 Kyiv, Ukraine

⁴ Institute for Condensed Matter Physics, Technical University Darmstadt, 64289 Darmstadt, Germany; miller@fkp.tu-darmstadt.de (R.M.)

* Correspondence: giuseppe.loglio@ge.icmate.cnr.it (G.L.), vladim@koyal.kiev.ua (V.I.K.)

S1. Comparison of the FMM model's predictions with those of the Lucassen and van den Tempel model (LvT model)

Below, in Figures S1-S5 the modulus and phase shift of the surface dilational viscoelasticity of ethyl lauroyl arginate (LAE) solutions, measured at different concentrations ($c = 0.1$ mM, 0.2 mM, 0.3 mM, 0.5 mM, and 0.8 mM), are compared with predictions of the LvT model and the FMM model.

The fitting parameters are reported in Table S1 for the LvT model and for the single FMM model as a function of concentration.

Table S1. Best fit parameters of the LvT model and of the single FMM model for the modulus and phase shift of the complex surface dilational viscoelasticity of LAE solutions.

| Concentration [mM] | LvT model | | Single FMM model | | |
|--------------------|---------------------|--------------------|------------------|------------|--------------|
| | ϵ_0 [mN/m] | ω_D [rad/s] | E [mN/m] | τ [s] | α [-] |
| 0.1 | 30.95 | 0.007 | 51.2 | 3.59 | 0.2 |
| 0.2 | 34.01 | 0.026 | 64.1 | 0.3 | 0.21 |
| 0.3 | 78.64 | 0.089 | 195.2 | 0.042 | 0.27 |
| 0.5 | 46.58 | 0.030 | 84.16 | 0.62 | 0.28 |
| 0.8 | 28.51 | 0.096 | 54.94 | 0.36 | 0.42 |

Note: The parameters of the LvT model are different from those presented in ref.[1] because they were varied here to fit also the phase shift, which was not considered in the original publication.

The real and imaginary parts of the complex surface dilational viscoelasticity $\epsilon^*(i\omega)$ for the LvT model are given by the following equations:

$$\epsilon_r = \epsilon_0 \times \frac{1 + \sqrt{\omega_D / \omega}}{1 + 2\sqrt{\omega_D / \omega} + 2\omega_D / \omega} \quad (S1)$$

$$\epsilon_i = \epsilon_0 \times \frac{\sqrt{\omega_D / \omega}}{1 + 2\sqrt{\omega_D / \omega} + 2\omega_D / \omega} \quad (S2)$$

where ϵ_0 and ω_D are the model parameters. Accordingly, the modulus and phase-shift of the complex function $\epsilon^*(i\omega)$ for LvT model are given by:

$$|\epsilon^*(i\omega)| = \frac{\epsilon_0}{\sqrt{1 + 2(\omega_D/\omega)^{0.5} + 2\omega_D/\omega}} \tag{S3}$$

$$\phi = 57.29578 \times \arctan(\epsilon_i/\epsilon_r) \tag{S4}$$

The real and imaginary parts of the complex surface dilational viscoelasticity $\epsilon^*(i\omega)$ for the single FMM model are given by the following equations:

$$\epsilon_r = E \times \frac{(\tau\omega)^{2\alpha} + (\tau\omega)^\alpha \cos(\pi\alpha/2)}{1 + (\tau\omega)^{2\alpha} + 2(\tau\omega)^\alpha \cos(\pi\alpha/2)} \tag{S5}$$

$$\epsilon_i = E \times \frac{(\tau\omega)^\alpha \sin(\pi\alpha/2)}{1 + (\tau\omega)^{2\alpha} + 2(\tau\omega)^\alpha \cos(\pi\alpha/2)} \tag{S6}$$

where E, τ and α are the model parameters. The modulus and phase shift of the complex function $\epsilon^*(i\omega)$, for a single-element fractional Maxwell model, also read:

$$|\epsilon^*(i\omega)| = E \times \frac{(\tau\omega)^\alpha}{\sqrt{1 + (\tau\omega)^{2\alpha} + 2(\tau\omega)^\alpha \cos(\pi\alpha/2)}} \tag{S7}$$

$$\phi = 57.29578 \times \arctan(\epsilon_i/\epsilon_r) \tag{S8}$$

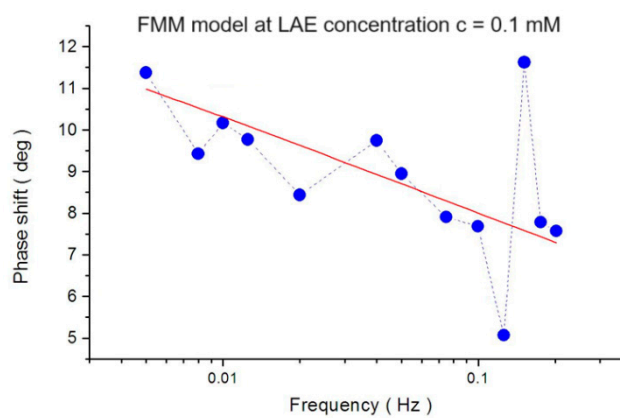
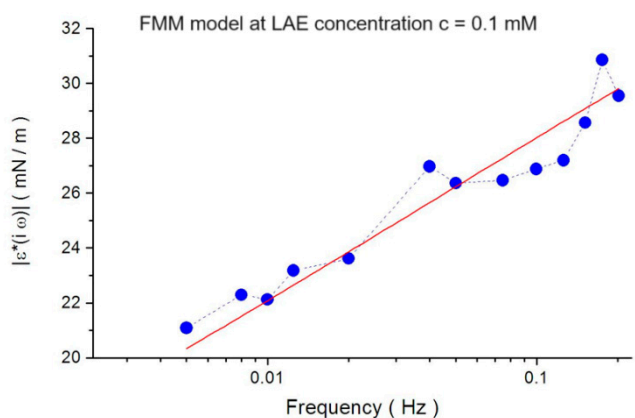
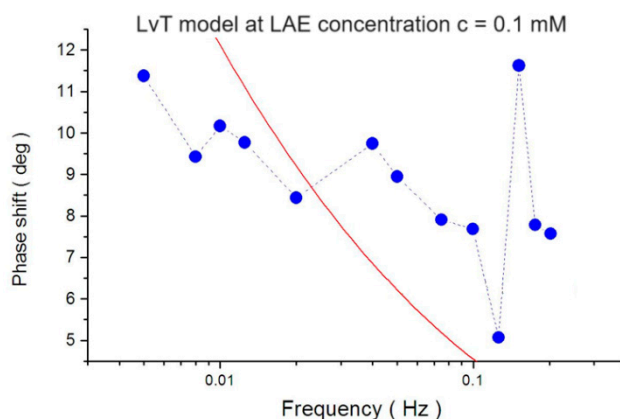
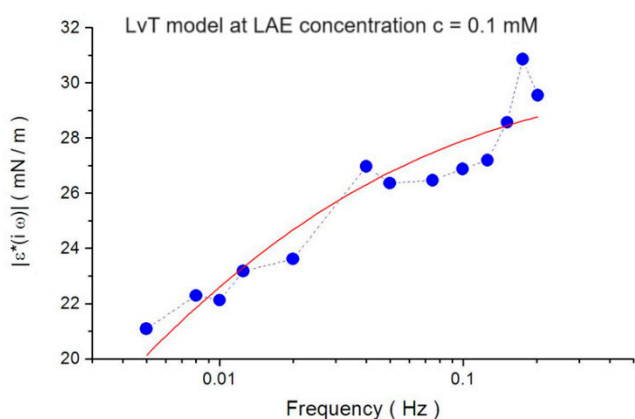


Figure S1. Frequency dependence of the modulus and phase shift of the complex physical quantity $\varepsilon^*(i\omega)$, measured at LAE concentration $c = 0.1$ mM. The lines are the results of calculations using the LvT model (top) and FMM model (bottom) with the parameter sets reported in Table S1.

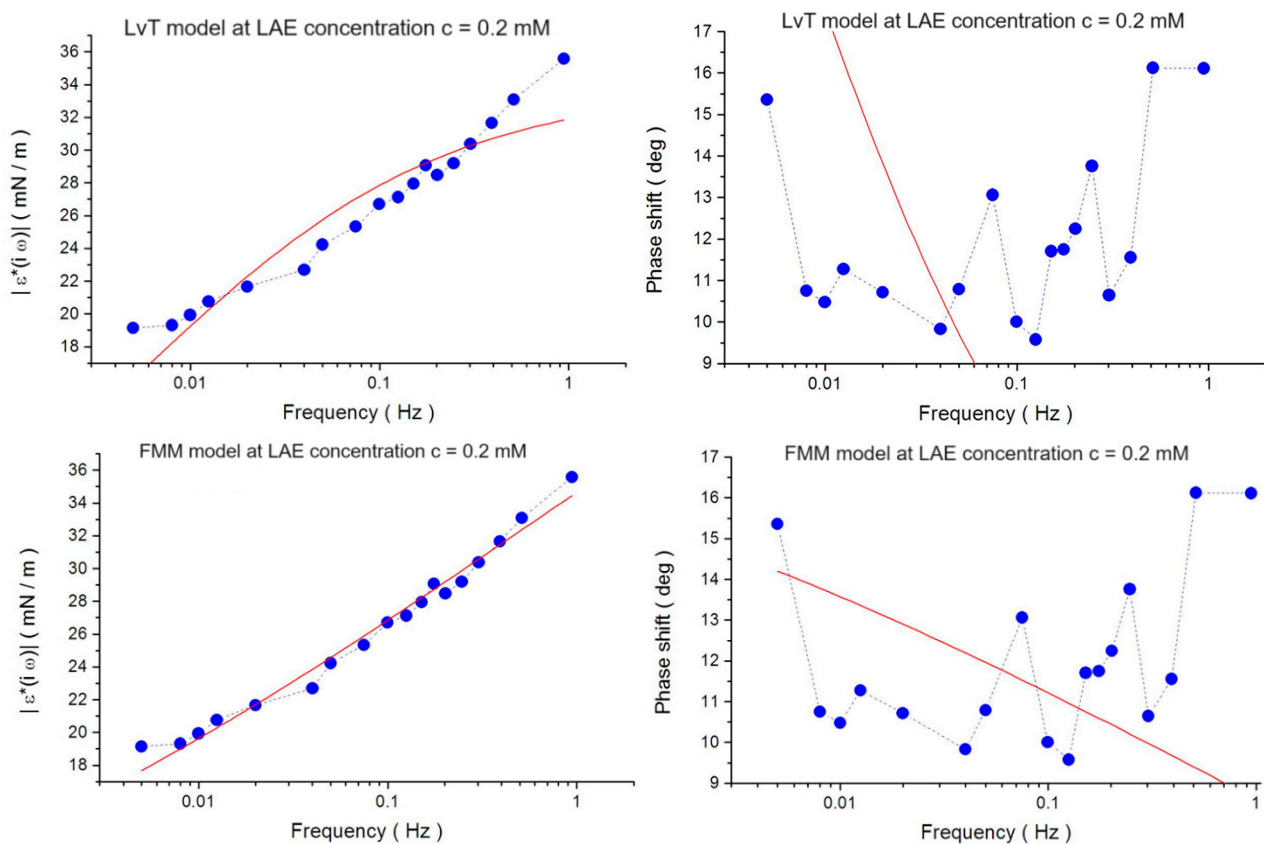
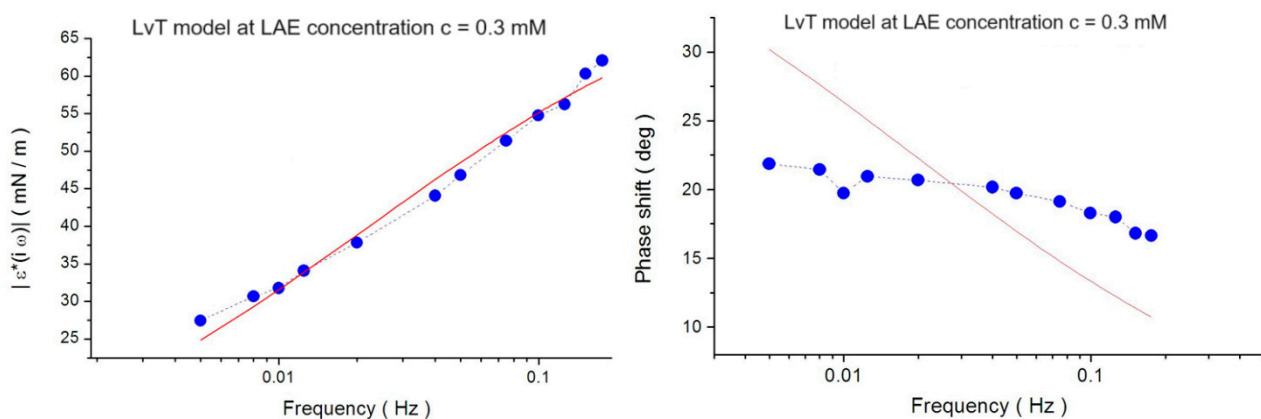


Figure S2. Frequency dependence of the modulus and phase shift of the complex physical quantity $\varepsilon^*(i\omega)$, measured at LAE concentration $c = 0.2$ mM. The lines are the results of calculations using the LvT model (top) and FMM model (bottom) with the parameter sets reported in Table S1.



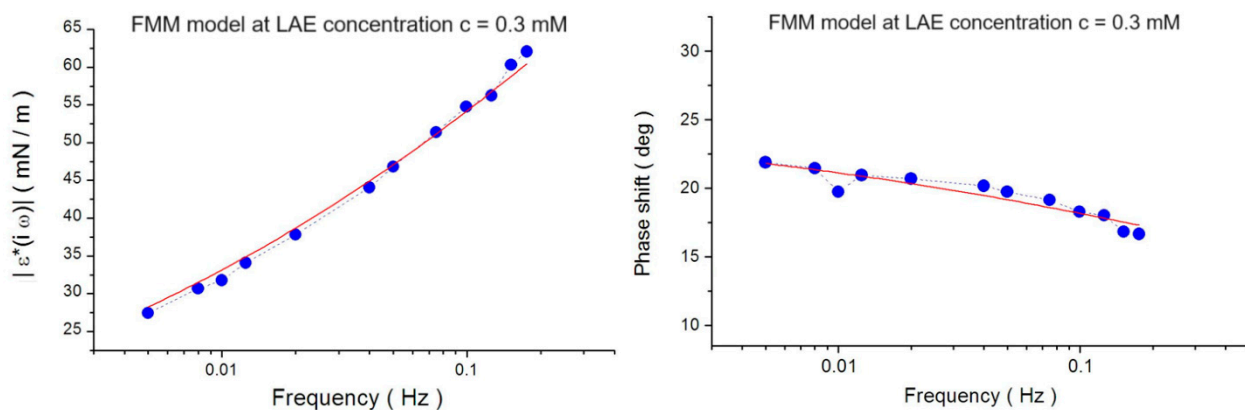


Figure S3. Frequency dependence of the modulus and phase shift of the complex physical quantity $\varepsilon^*(i\omega)$, measured at LAE concentration $c = 0.3$ mM. The lines are the results of calculations using the LvT model (top) and FMM model (bottom) with the parameter sets reported in Table S1.

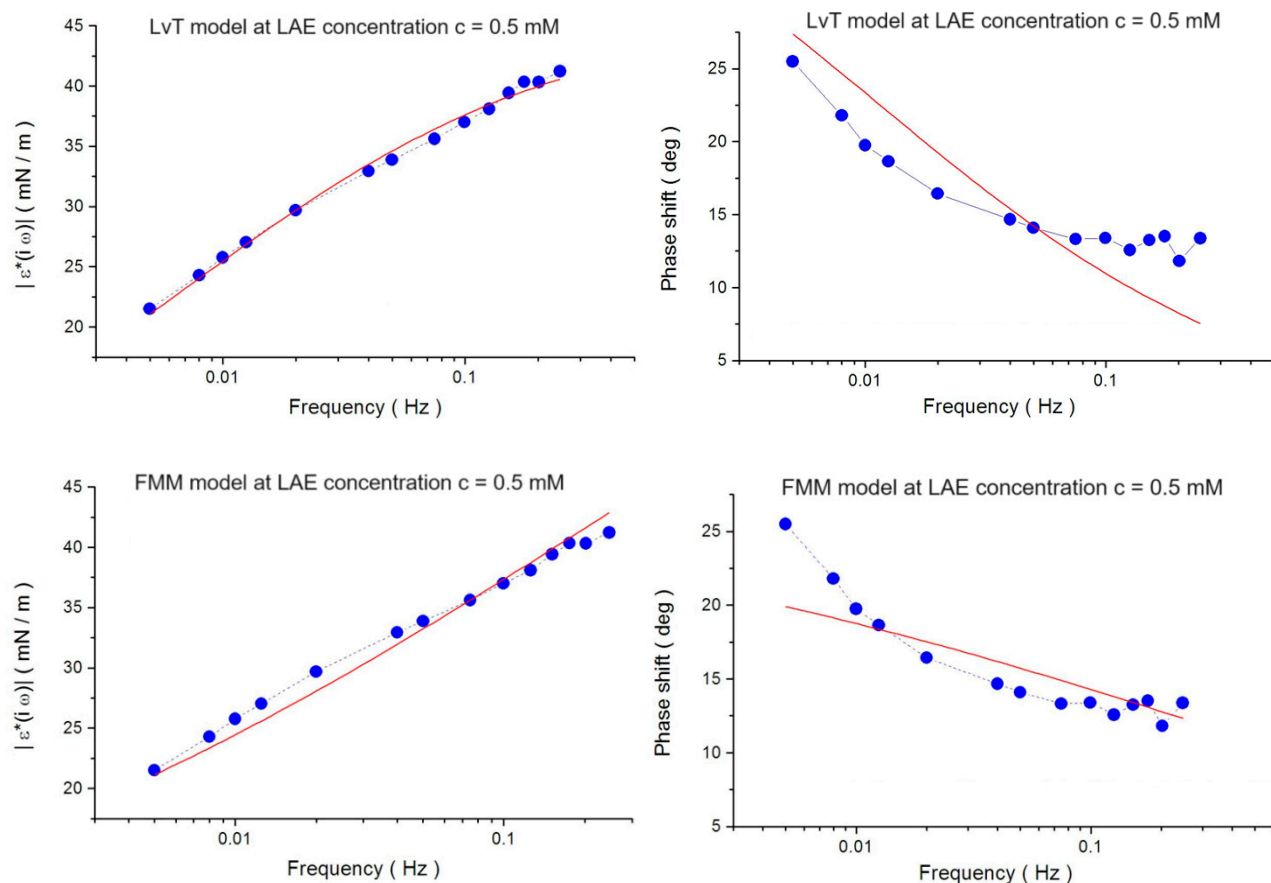


Figure S4. Frequency dependence of the modulus and phase shift of the complex physical quantity $\varepsilon^*(i\omega)$, measured at LAE concentration $c = 0.5$ mM. The lines are the results of calculations using the LvT model (top) and FMM model (bottom) with the parameter sets reported in Table S1.

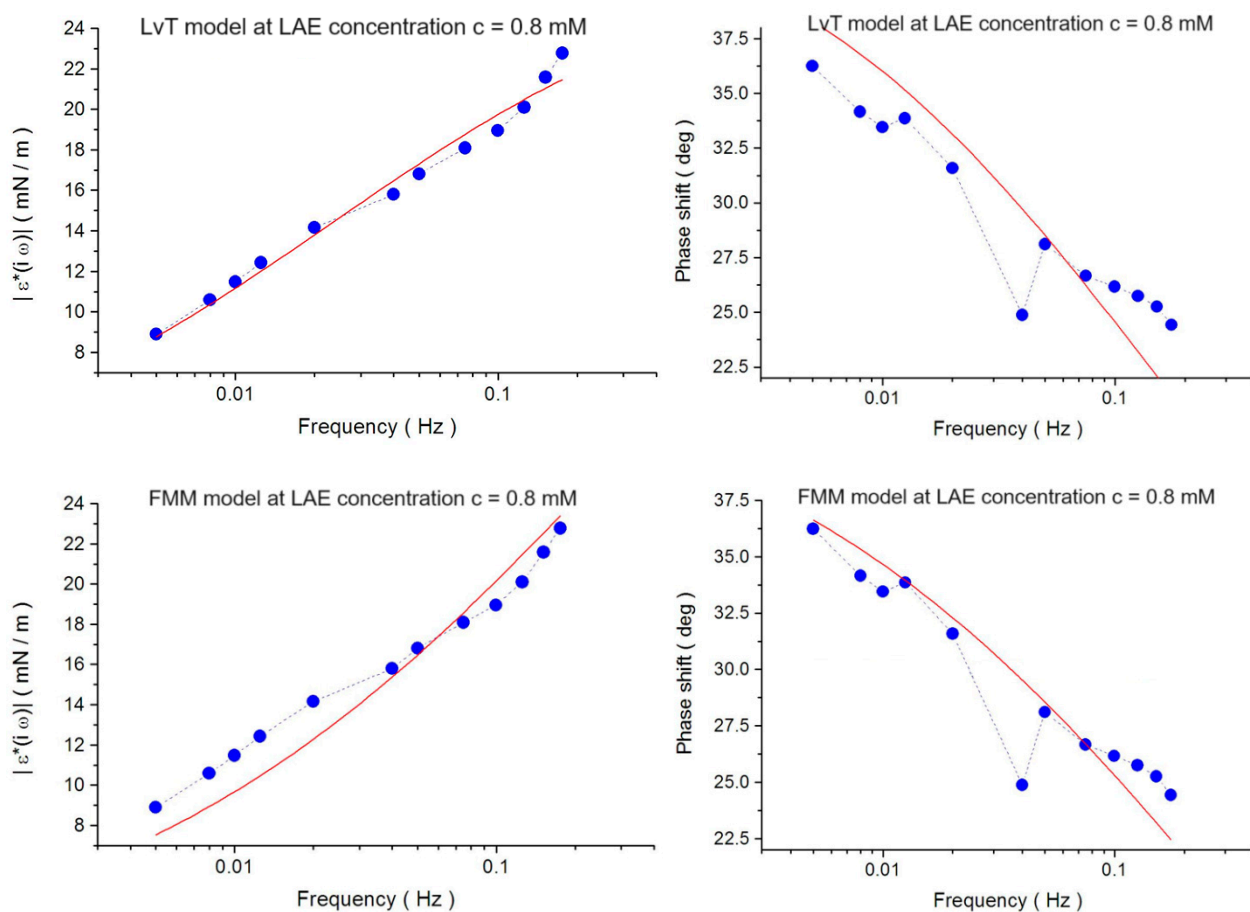


Figure S5. Frequency dependence of the modulus and phase shift of the complex physical quantity $\varepsilon^*(i\omega)$, measured at LAE concentration $c = 0.8$ mM. The lines are the results of calculations using the LvT model (top) and FMM model (bottom) with the parameter sets reported in Table S1.